

## Potential of Wind Energy Development for Water Pumping in Ngaoundere

Ruben M. Mouangue<sup>1\*</sup>, Myrin Y. Kazet<sup>1,2</sup>, Daniel Lissouck<sup>3</sup>, Alexis Kuitche<sup>2</sup> and J.M. Ndjaka<sup>4</sup>

<sup>1</sup>Department of Energetic Engineering, UIT, University of Ngaoundere, Cameroon

<sup>2</sup>Departments of GEEA, PAI, ENSAI, University of Ngaoundere, Cameroon

<sup>3</sup>Department of Renewable Energy, HTTTC, Kumba, Cameroon

<sup>4</sup>Department of Physics, Faculty of Sciences, University of Yaounde 1, Cameroon

### Abstract

The modelling of wind energy conversion systems is of great importance if one intends to develop water pumping applications for a sustainable development. This paper presents a technical assessment based on the measured wind data in which we investigate the possibility of coupling piston pump, roto-dynamic pump and electric pump with wind rotors for water pumping applications. Weibull distribution is used to model the monthly mean wind speed for a location in the town of Ngaoundere. It is found that there is a good agreement between the predicted values of the mean wind speed and those obtained from data suggesting that the Weibull distribution can be used to provide accurate estimation of the mean wind speed. The mean electric power and energy are computed based on the power curves of Vestas V25 and V100. Taking into account the wind regime characteristics of our site, we provide the amount of water which can be expected from each type of wind pumps. The monthly amount of water has minimum and maximum average values of 422 m<sup>3</sup> and 674 m<sup>3</sup> for the piston pump, 1275 m<sup>3</sup> and 1982 m<sup>3</sup> for the roto-dynamic pump and 31334 m<sup>3</sup> and 100042 m<sup>3</sup> for the electric pump. From the results, it is clear that electric pump offer better performances than piston and roto-dynamic pumps.

**Keywords:** Weibull distribution; Wind power; Water pumping; Ngaoundere

### Abbreviations:

C<sub>p</sub>: Power coefficient; g: Acceleration due to gravity, m.s<sup>-2</sup>; H: Head of water, m; Q: Water flow rate, m<sup>3</sup>.h<sup>-1</sup>; η: Efficiency of transmission; f (V): Probability density function of the Weibull distribution; F (V): Cumulative distribution function; Γ ( ): Gamma function; QVE: Instantaneous discharge of the electric pump, m<sup>3</sup>.s<sup>-1</sup>; V<sub>m</sub>: Mean wind speed, m.s<sup>-1</sup>; G: Gear ratio; λd: Design tip ratio; DT: Rotor diameter, m; PR: Rated power, W; Npd: Pump speed at design point, rps; UN: United Nations; ρ<sub>a</sub>: Air density, kg.m<sup>-3</sup>; ρ<sub>w</sub>: Water density, kg.m<sup>-3</sup>; k: Weibull shape parameter; C: Weibull scale parameter, m.s<sup>-1</sup>; V: Instantaneous wind speed, m.s<sup>-1</sup>; QVP: Instantaneous discharge of the piston pump, m<sup>3</sup>.s<sup>-1</sup>; PH: Hydraulic power, W; PV: Developed power, W; QVR: Instantaneous discharge of the roto-dynamic pump, m<sup>3</sup>.s<sup>-1</sup>; T: Time, s; V<sub>I</sub>: Cut-in wind speed, m.s<sup>-1</sup>; V<sub>O</sub>: Cut-out wind speed, m.s<sup>-1</sup>; V<sub>R</sub>: Rated velocity, m.s<sup>-1</sup>; V<sub>d</sub>: Design wind velocity, m.s<sup>-1</sup>; A: Swept surface, m<sup>2</sup>

### Introduction

In sub-Saharan Africa, operation and control of water in both rural and urban areas have become strategic issues for population growth, diversification of economic activities and the current degradation of the environment. Sensitive and complex subject, water should be open to all without any distinction but there is however still in 2015, a severe water crisis in Africa [1]. This is the continent where access to quality water is more limited, according to the 4<sup>th</sup> UN report on water [1]. Nevertheless, Africa has seventeen major rivers and hundreds of lakes, as well as significant groundwater. Despite all the efforts consent by the governments of African countries, it is clear that much remains to be done in terms of investment.

One of the solutions proposed to solve this problem could be to invest in the acquisition of infrastructures for pumping and water distribution. But first, we should carry out technical studies to provide effective assistance to investors as to the decisions concerning the planning and implementation of projects to supply drinking water.

Wind energy, which since 2009 is the second global source of renewable energy [2], remains unexploited in Cameroon. The wind pumping could be an interesting solution for people in rural areas because it uses a free energy source and does not contribute to increased greenhouse gas emissions [3].

In this paper, we investigate the possibility of coupling piston pump, roto-dynamic pump and electric pump with wind rotors for water pumping applications.

Although the performance of piston and wind-driven roto-dynamic pumps were estimated in some studies as the one of Mathew and Pandey in 2003 [4], the distribution of wind speed in a regime was modelled by using the Rayleigh distribution which is a particular case of the Weibull distribution and has not yet been investigated for the site of Ngaoundere. However, the Weibull distribution has been found satisfactory for the modelling of the observable wind speed frequency in general [5-7] and for the case of Ngaoundere site in particular [8]. Approximation which consists of assuming that the variation between two nodes of the power-wind speed curve is linear is also considered here for the computation of pumped volume flow rate of an electric pump. Taking into account the wind regime characteristics of our site, we provide the amount of water which can be expected from each type of wind pumps and we compare them.

**\*Corresponding author:** Ruben M. Mouangue, Department of Energetic Engineering, UIT, University of Ngaoundere, P. O Box 455, Ngaoundere, Cameroon, Tel: 237 677 46 10 06; E-mail: [r\\_mouangue@yahoo.fr](mailto:r_mouangue@yahoo.fr)

**Received** October 19, 2015; **Accepted** December 10, 2015; **Published** December 14, 2015

**Citation:** Mouangue RM, Kazet MY, Lissouck D, Kuitche A, Ndjaka JM (2015) Potential of Wind Energy Development for Water Pumping in Ngaoundere. J Fundam Renewable Energy Appl 6: 198. doi:10.4172/20904541.1000198

**Copyright:** © 2015 Mouangue RM, et al. This is an open-access article distributed under the terms of the Creative Commons Attribution License, which permits unrestricted use, distribution, and reproduction in any medium, provided the original author and source are credited.

## Material and Methods

### Weibull distribution

The probability density function (PDF) of the Weibull distribution is used to characterize the frequency distribution of wind speeds over time and is expressed mathematically as [5,6]:

$$f(V) = \frac{k}{C} \left(\frac{V}{C}\right)^{k-1} \exp\left[-\left(\frac{V}{C}\right)^k\right] \quad (1)$$

This distribution is characterized by two parameters: a dimensionless shape parameter  $k$  and a scale parameter  $C$  (m/s).

The cumulative distribution function (CDF) is expressed in equation 2 as [6,9]:

$$F(V) = 1 - \exp\left[-\left(\frac{V}{C}\right)^k\right] \quad (2)$$

### Mean wind speed

One of the most important wind characteristics is the mean wind speed. The probability density function and Weibull parameters are related to the mean speed by equation 3 [5,9].

$$V_m = C \tilde{\Lambda} \left(1 + \frac{1}{k}\right) \quad (3)$$

Where

$$\tilde{\Lambda}(n) = \int_0^{\infty} x^{n-1} e^{-x} dx \quad (4)$$

$\Gamma(\cdot)$  is the gamma function.

### Extrapolation of weibull parameters

Most modern wind turbines have hub heights considerably higher than measurement heights of meteorological towers. Hence, the measured wind characteristics at the lower measurement height must be extrapolated to the hub height of the turbine. For this task we choose the use of the Justus and Mikhail law [6,9,10]. The values of Weibull's parameters ( $k_h$  and  $C_h$ ) are then evaluated at any desired height ( $Z_h$ ) by the following equations (5) and (6):

$$k_h = k_a \left[1 - ALn \left(\frac{Z_h}{Z_a}\right)\right]^{-1} \quad (5)$$

$$C_h = C_a \left(\frac{Z_h}{Z_a}\right)^n \quad (6)$$

The exponent  $n$  is expressed as:

$$n = B - ALn C_a \quad (7)$$

Where constants  $A = 0.0881$  and  $B = 0.37$ .

$k_a$  and  $C_a$  are, respectively, the shape parameter and the scale parameter at the anemometer height  $Z_a = 10$  m.

### Wind pump discharges

**Piston pump:** Piston pumps are types of pump with reciprocating motion. The overall performance coefficient of a wind rotor coupled to a reciprocating pump can be modelled as [11]:

$$C_p \eta = 4C_{pd} \eta(T, P) \left[1 - K_o \left(\frac{V_l}{V}\right)^2\right] K_o \left(\frac{V_l}{V}\right)^2 \quad (8)$$

where  $C_p \eta$  is the overall (wind to water) efficiency of the system,  $C_{pd}$  is the power coefficient of the rotor at the design point,  $\eta(T, P)$  is the combined transmission and pump efficiency and  $K_o$  is a constant taking care of the starting behaviour of the rotor pump combination.

The power developed by the system in pumping water  $P_v$  is given by equation (9).

$$P_v = \frac{1}{2} C_p \eta \rho_a A V^3 \quad (9)$$

From Equations (8) and (9),  $P_v$  can be expressed as:

$$P_H = \rho_w g Q_{VP} H \quad (10)$$

The hydraulic power  $P_{HP}$  needed by the pump for delivering a discharge of  $Q_{VP}$  against a head  $H$  is estimated by the equation below:

$$P_H = \rho_w g Q_{VP} H \quad (11)$$

By equalizing  $P_H$  and  $P_v$ , the instantaneous discharge  $Q_{VP}$  of the system at any velocity  $V$  can be deduced.

$$Q_{VP} = 2C_{pd} \eta(T, P) \frac{\rho_a}{\rho_w} \frac{\pi D_T^2}{4gH} V^3 \left[1 - K_o \left(\frac{V_l}{V}\right)^2\right] K_o \left(\frac{V_l}{V}\right)^2 \quad (12)$$

The wind regime characteristics are integrated with the model in order to provide the pumped volume flow rate expected over a time period.

$$Q_p = T \int_{V_i}^{V_o} Q_{VP}(V) f(V) dV \quad (13)$$

$f(V)$  is the probability density function of the Weibull distribution.  $V_i$  and  $V_o$  are respectively cut-in wind speed and cut-out wind speed.

The pumped volume flow rate expected from a wind driven piston pump, installed at a given site, over a period  $T$  is obtained by computing equation (14).

$$Q_p = 2C_{pd} \eta(T, P) \frac{\rho_a}{\rho_w} \frac{\pi D_T^2}{4gH} T \int_{V_i}^{V_o} \left[1 - K_o \left(\frac{V_l}{V}\right)^2\right] K_o \left(\frac{V_l}{V}\right)^2 \left(\frac{k}{C}\right) \left(\frac{V}{C}\right)^{k-1} \exp\left[-\left(\frac{V}{C}\right)^k\right] dV \quad (14)$$

**Roto-dynamic pump:** According to the paper of Mathew and Pandey [4], the discharge of an ideal roto-dynamic pump at any speed  $V$  can be estimated by using the equation (15) below:

$$Q_{VR} = \frac{1}{8} C_{pd} \eta_{pd} D_T \frac{\rho_a}{\rho_w} \frac{V_d^3}{gH} \frac{G \lambda_d}{N_{pd}} V \quad (15)$$

Where  $C_{pd}$  is the design power coefficient,  $\eta_{pd}$  is efficiency,  $D_T$  is the diameter of the rotor,  $G$  is the gear ratio,  $\lambda_d$  is the design tip ratio,  $N_{pd}$  is the pump speed at design point and  $V_d$  is the design wind velocity.

If we integrate the wind regime characteristics with the model, the output providing the pumped volume flow rate expected over a time period from a wind-powered water pumping system at a given site can be expressed by equation (16):

$$Q_R = T \int_{V_i}^{V_o} Q_{VR}(V) f(V) dV \quad (16)$$

From equation (15) and (16), the integrated system output can be expressed as:

$$Q_R = \frac{1}{8} k C_{pd} \eta_{pd} D_T \frac{\rho_a}{\rho_w} \frac{V_d^3}{gH} \frac{G \lambda_d}{N_{pd}} T \int_{V_i}^{V_o} \left(\frac{V}{C}\right)^k \exp\left[-\left(\frac{V}{C}\right)^k\right] dV \quad (17)$$

The integrated output of the roto-dynamic pump is then estimated by the computation of equation (17).

**Electric pump:** To estimate the discharge of an electric pump, the power developed by the wind turbine generator  $P(V)$  may be equated with the corresponding hydraulic power  $P_H$  demand.

$$P_H = \frac{\rho_w g Q_{VE} H}{\eta} = P(V) \quad (18)$$

Hence, discharge of the pump at any speed  $V$  can be expressed as follow:

$$Q_{VE} = \frac{\eta}{\rho_w g H} P(V) \quad (19)$$

Where  $P(V)$  is the electric power generated at a given speed  $V$ .

Values of  $P(V)$  are provided by the manufacturer of the wind turbine generator through the power curve.

In this work, we have made the choice of two power curves: Vestas V82 [12] with a hub height of 40 m (Figure 1) and Vestas V100 [13] with a hub height of 80 m (Figure 2) because of their relatively low cut-in wind speed (Table 1).

It is possible to carry out an approximation which consists of assuming that the variation between two nodes of the power-wind speed curve is linear [14]. Then, given two points  $i$  and  $i + 1$  of the power curve, power as a function of speed can be written as equation (20).

$$P(V) = \frac{P_{i+1} - P_i}{V_{i+1} - V_i} (V - V_i) + P_i \quad (20)$$

By using this approximation, power curves of both wind turbines is plotted as shown in Figures 1 and 2.

Then, the amount of water expected over a time period is obtained by integrating the wind regime characteristics into the electric pump discharge equation.

$$Q_E = T \int_{V_i}^{V_o} Q_{VE} f(V) dV \quad (21)$$

By substituting equation (19) in (21) we have:

$$Q_E = \frac{\eta T}{\rho_w g H} \int_{V_i}^{V_o} P(V) f(V) dV \quad (22)$$

Substituting equation (1) and (20) in (22), the pumped volume flow rate of an electric pump is then estimated by solving numerically equation (23) below:

$$Q_E = \frac{\eta T}{\rho_w g H} \left[ \int_{V_i}^{V_{i+1}} \frac{P_{i+1} - P_i}{V_{i+1} - V_i} (V - V_i) + P_i \left( \frac{k}{C} \right) \left( \frac{V}{C} \right)^{k-1} \exp \left[ - \left( \frac{V}{C} \right)^k \right] dV + P_{i+1} \left( \frac{k}{C} \right) \left( \frac{V}{C} \right)^{k-1} \exp \left[ - \left( \frac{V}{C} \right)^k \right] dV \right] \quad (23)$$

In the present study, the computation of equations was made through Fortran codes that we wrote using for this task Eclipse Juno which is an open source integrated development environment [15]. Specifications of the three systems considered for the analysis are given in (Table 1) [4].

## Results and Discussion

Results of Ngaoundere wind resource analysis using one year wind data as well as the vertical wind shear analysis and the water discharge at various wind turbine hub heights are given in this section.

### Monthly wind speed variation

Monthly mean wind speed variation is found in the range 1.292-1.794 m/s as shown in Figure 3. The lowest wind speed of 1.292 m/s occurs in October and the highest wind speed 1.794 m/s in February. The maximum monthly mean wind speeds occur during February, March and May with 1.794 m/s, 1.786 m/s and 1.788 m/s, respectively. Wind speeds decrease to 1.292 m/s in October and slightly gain strength as 1.470 m/s, 1.523 m/s, and 1.576 m/s during November, December and January, respectively.

In Figure 3, the predicted values of the mean wind speed are plotted side by side to those obtained from data. As we can see, there is a good agreement between them. It suggests that the Weibull distribution can be used to provide accurate estimation of the mean wind speed.

### Observed wind speed histogram

The observed wind speed histogram is well approximated by the Weibull probability density function. This is shown by Figure 4. The

Pearson's correlation coefficient computed is 0.9 suggesting that the wind regime of a site can be well described by the Weibull distribution.

### Wind regime at different heights

After the Weibull parameters have been extrapolated at 40 m and 80 m heights, probability density functions using only global values for each of them are plotted side by side in Figure 5.

Cumulative distribution functions for the whole year of the site are also plotted at different altitudes. This is shown in Figure 6.

The trend regarding the evolution of the PDF curve function of altitude (Figure 5) is similar to that obtained by Safari and Gasore [16]. This trend reflects the fact that the probability of significant wind increases with altitude. The trend is the same for CDF curves shown in Figure 6.

### Wind speed shear analysis

The vertical wind profile is calculated at hub heights of wind turbines at 40 m and 80 m from one year data. The monthly mean wind speed variations at different hub heights are shown in Figure 7.

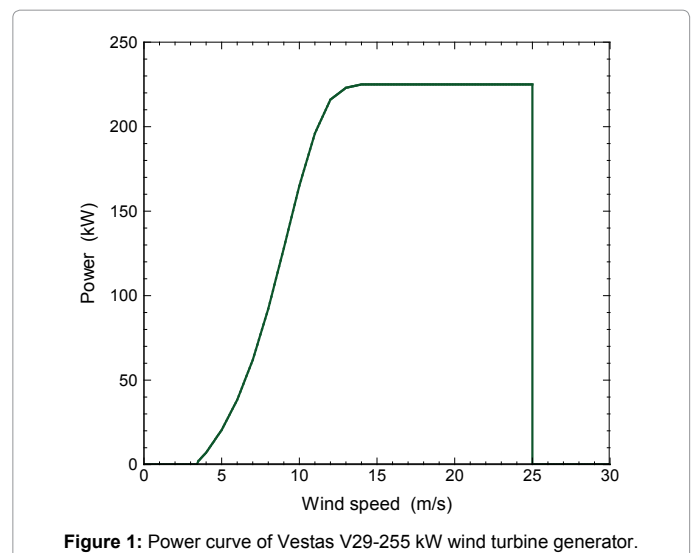


Figure 1: Power curve of Vestas V29-255 kW wind turbine generator.

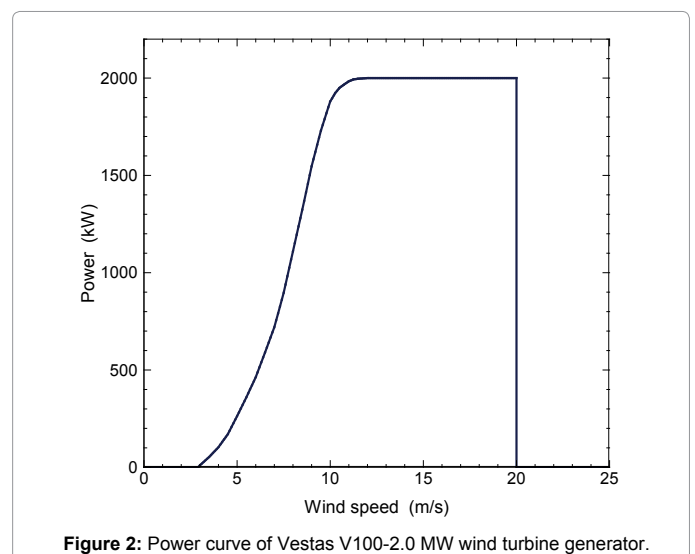
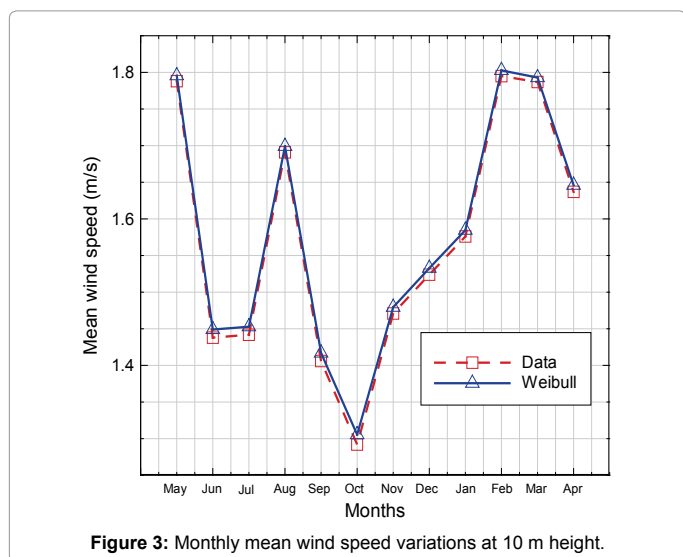


Figure 2: Power curve of Vestas V100-2.0 MW wind turbine generator.

Pump specifications	Piston	Roto-dynamic	Electric	
			V29	V100
Coefficient K	0.25	-		-
Cut-in wind speed (m/s)	2.5	2.5	3	3.5
Cut-out wind speed (m/s)	10	10	20	25
Design power coefficient	0.3	0.38		
Design tip speed ratio	-	2		-
Design wind velocity	-	6		-
Efficiency (pump + transmission)	0.95	0.558		
Gear ratio	-	19.8		-
Rated power			255 kW	2000 kW
Rated wind speed			14 m/s	12 m/s
Pump speed at design point (rps)	-	40		-

**Table 1:** Specifications of the three wind-driven pumps considered for the performance computation.



**Figure 3:** Monthly mean wind speed variations at 10 m height.

The monthly reference mean wind speeds during the period May 2011 to April 2012 vary from 1.292 m/s to 1.794 m/s which is increased from 2.762 m/s to 3.772 m/s at the 80 m hub height in October and February.

These wind speeds are found to be suitable for micro wind turbines with lower cut-in speeds. The one year extrapolated wind speeds at this location at 40 m height are not found suitable for large turbines for electricity power generation as they require at least annual mean wind speeds of 3-7 m/s. Figure 8 shows that at some hours of the day, the wind speed is higher than the cut-in wind speed. The wind turbine for this period will be able to produce electricity to supply the pumps and to recharge batteries.

### Monthly power and Energy output

The monthly and annual electric power developed  $P_u$  and energy  $E$  is calculated and the results are shown in Table 2.

At 40 m height, the maximum value of monthly mean electric power is computed as 14.04 kW in March and the minimum value is computed as 4.40 kW in October. However, the monthly energy has maximum average value of 10.453 MWh in March while the minimum value is obtained as 3.274 MWh in October.

At 80 m height, the maximum and the minimum values of the monthly mean electric power are respectively 287.94 kW in February and 123.70 kW in October while the monthly energy has maximum

and minimum average values of 213.471 MWh in March and 92.036 MWh in October, respectively.

It can be also observed from Table 2 that the power generated by the wind turbine increases with altitude. This result confirms the trend observed above that the probability of significant wind increases with altitude. Thus, the wind resource becomes increasingly important when the altitude increases.

### Monthly and annual water output

Results obtained from the computation of volume flow rate equations are shown in Table 3. It presents the monthly and annual volume flow rate and amount of water for the three types of pump considered at the same height.

For the piston pump, the maximum value of the volume flow rate is computed as  $0.917 \text{ m}^3\text{h}^{-1}$  in February and the minimum value is computed as  $0.567 \text{ m}^3\text{h}^{-1}$  in October. However, the monthly amount of water has maximum average value of  $674 \text{ m}^3$  in March while the minimum value is obtained as  $422 \text{ m}^3$  in October.

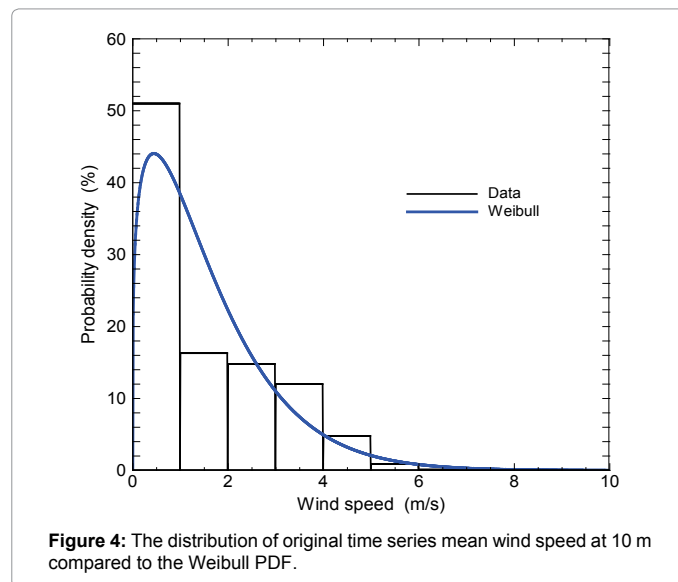


**Figure 4:** The distribution of original time series mean wind speed at 10 m compared to the Weibull PDF.

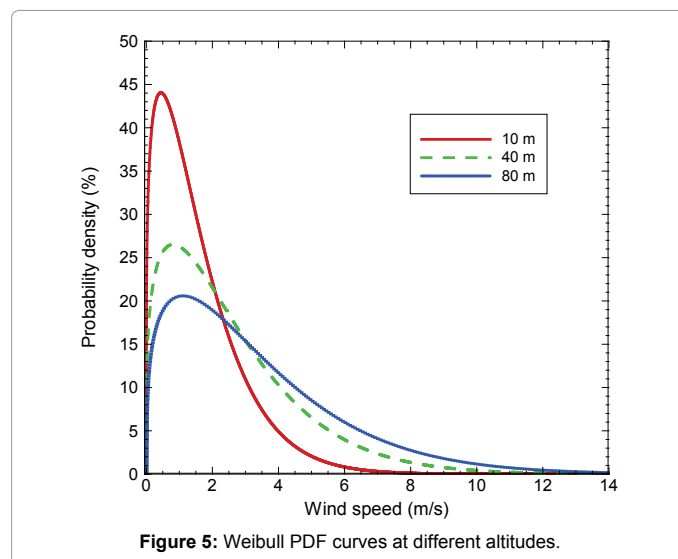


**Figure 5:** Weibull PDF curves at different altitudes.

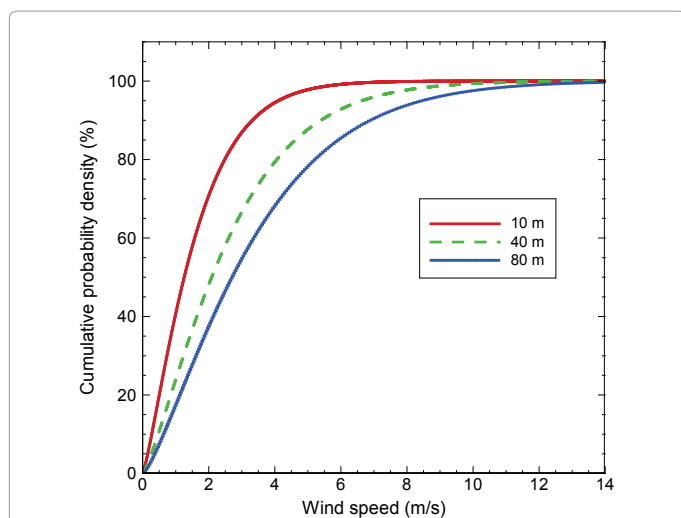


Figure 6: Weibull cumulative distribution function curves at different altitudes.

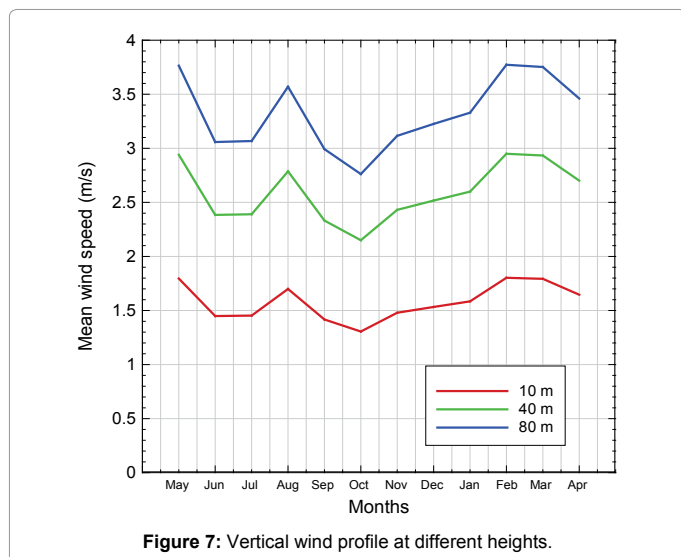


Figure 7: Vertical wind profile at different heights.

Then, the roto-dynamic pump has  $2.700 \text{ m}^3\text{h}^{-1}$  and  $1.713 \text{ m}^3\text{h}^{-1}$  as maximum and minimum values of the volume flow rate, respectively. On the other hand, it has  $1982 \text{ m}^3$  and  $1275 \text{ m}^3$  as maximum and minimum values of the amount of water, respectively for the same months as above.

For the electric pump finally, the maximum and the minimum values of the volume flow rate are respectively  $134.465 \text{ m}^3\text{h}^{-1}$  in March and  $42.116 \text{ m}^3\text{h}^{-1}$  in October while the monthly amount of water has maximum and minimum average values of  $100042 \text{ m}^3$  in March and  $31334 \text{ m}^3$  in October, respectively.

As a result of (Table 3), monthly pumped volume flow rate and water amount at 40 m height of piston, roto-dynamic and electric pumps are plotted in Figures 9 and 10. It can be seen that the rate of discharge patterns are similar to each other. By looking at Figure 8 it is clear that at the same height, the monthly discharge rate of the electric pump is upper than the one of roto-dynamic pump which is itself upper than the piston one. One can also note that an important gap exists between the volume flow rate of the electric pump and the two other types of pump. On the other hand, it is less important between

volume flow rates of piston and roto-dynamic pumps. In the months of May, Aug, Feb, Mar and Apr monthly mean wind speeds are upper than  $2.7 \text{ m/s}$  and therefore more wind energy can be captured by wind turbines and pumped water flows rates are consequent.

Monthly water amount histogram is found in the ranges  $422 - 674 \text{ m}^3$  for the piston pump,  $1275 - 1982 \text{ m}^3$  for the roto-dynamic pump and  $31334 - 100042 \text{ m}^3$  for the electric pump as shown in Figure 9. The lowest amount occurs in October and the highest amount in March.

At the same height, results show that electric pump offer better performances than piston and roto-dynamic pumps. Roto-dynamic and piston pumps are therefore recommend for low head of water.

In practice, piston and roto-dynamic pumps are located near water points. If the wind resource is not enough at the water point, there will be no good outputs. This disadvantage could be overcome by the use of an electric pump. The turbine being able to be installed far from the site of the pump, it could be therefore installed at the most important resource place. Furthermore, if storage devices like batteries are combined to the system, water could be pumped at any time of the day independently of the wind availability.

## Conclusion

In this study the potential of the development of water pumping using wind energy in Ngaoundere is carried out. Energy produced by the rotor in wind regimes following the Weibull distribution and the amount of water output from three types of pump are estimated. The most important outcomes of the study can be summarized as follows:

The monthly mean wind speeds are recorded as  $1.292$  and  $1.794 \text{ m/s}$  in October and February for the minimum and maximum values respectively at  $10 \text{ m}$  height; the monthly mean electric power and energy at  $40 \text{ m}$  height are computed as  $4.40 \text{ kW}$ ,  $3.274 \text{ MWh}$  in October and  $14.04 \text{ kW}$ ,  $10.453 \text{ MWh}$  in March for the minimum and maximum values. At  $80 \text{ m}$  height, these values are respectively  $123.70 \text{ kW}$ ,  $92.036 \text{ MWh}$  in October,  $287.94 \text{ kW}$  in February and  $213.471 \text{ MWh}$  in March. These wind speeds, power and energy are found to be suitable for micro wind turbines with lower cut in speeds.

There is a good agreement between the predicted values of the mean wind speed and those obtained from data suggesting that the

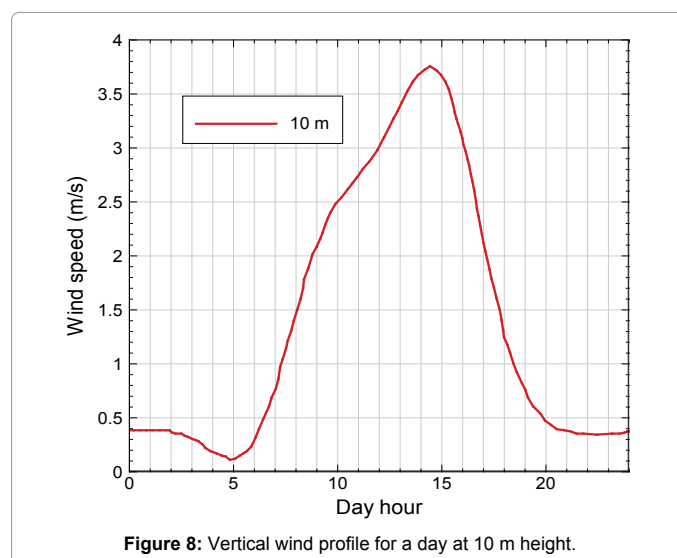


Figure 8: Vertical wind profile for a day at 10 m height.

Months	Wind Turbine Generators			
	Vestas V29 - 255 kW		Vestas V100 - 2 MW	
	40 m		80 m	
	Pu	E	Pu	E
	(kW)	(MWh)	(kW)	(MWh)
May-11	11.93	8.883	270.42	201.197
Jun-11	6.46	4.654	166.03	119.546
Jul-11	6.11	4.55	161.78	120.368
Aug-11	9.91	7.378	236.28	175.796
Sep-11	5.92	4.266	155.69	112.102
Oct-11	4.4	3.274	123.7	92.036
Nov-11	8.05	5.795	188.73	135.89
Dec-11	8.69	6.467	202.25	150.474
Jan-12	9.95	7.408	221.46	164.769
Feb-12	13.93	9.698	287.94	200.41
Mar-12	14.04	10.453	286.92	213.471
Apr-12	9.24	6.652	221.86	159.744
<b>Global</b>				
1 year	8.97	78.773	210.59	1849.83

Table 2: Monthly and annual electric power and energy at different altitudes.

Months	Piston pump		Roto-dynamic pump		Electric pump	
	QP (m <sup>3</sup> h <sup>-1</sup> )	Amount of water (m <sup>3</sup> )	QR (m <sup>3</sup> h <sup>-1</sup> )	Amount of water (m <sup>3</sup> )	QE (m <sup>3</sup> h <sup>-1</sup> )	Amount of water (m <sup>3</sup> )
May-11	0.941	700	2.781	2069	114.269	85016
Jun-11	0.683	492	2.046	1473	61.863	44542
Jul-11	0.684	509	2.054	1528	58.535	43550
Aug-11	0.875	651	2.596	1932	94.913	70615
Sep-11	0.657	473	1.973	1421	56.707	40829
Oct-11	0.567	422	1.713	1275	42.116	31334
Nov-11	0.705	507	2.098	1510	77.037	55467
Dec-11	0.743	553	2.21	1644	83.197	61899
Jan-12	0.776	577	2.3	1711	95.297	70901
Feb-12	0.917	638	2.7	1879	133.362	92820
Mar-12	0.905	674	2.664	1982	134.465	100042
Apr-12	0.833	600	2.477	1784	88.43	63670
<b>Global</b>						
1 year	0.779	6839	2.314	20324	85.827	753905

Table 3: Monthly and annual pumped volume flow rate and water amount for each type of pump at 40 m height.

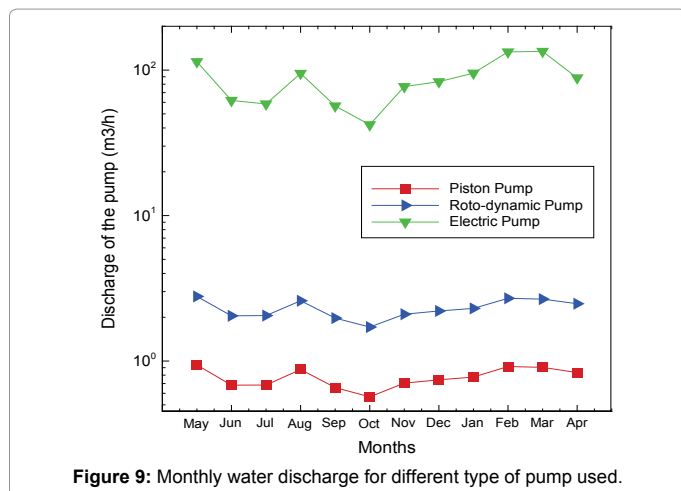


Figure 9: Monthly water discharge for different type of pump used.

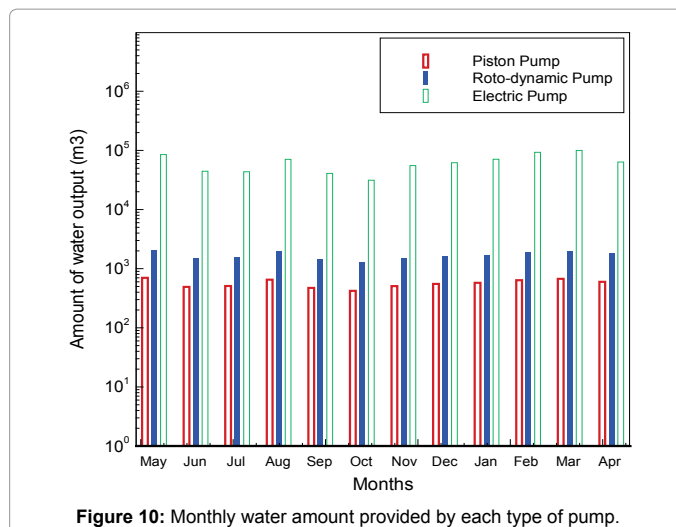


Figure 10: Monthly water amount provided by each type of pump.

Weibull distribution can be used to provide accurate estimation of the mean wind speed.

The monthly amount of water has minimum and maximum average values of 422 m<sup>3</sup> and 674 m<sup>3</sup> for the piston pump, 1275 m<sup>3</sup> and 1982 m<sup>3</sup> for the roto-dynamic pump and 31334 m<sup>3</sup> and 100042 m<sup>3</sup> for the electric pump.

At the same height, results show that electric pump offer better performances than piston and roto-dynamic pumps.

Underground water can be pumped using wind power and this could be an initial solution for people living in remote areas.

**Acknowledgments**

Authors would like to thank the ASECNA weather service of Ngaoundere for providing meteorological data used in this work. Thanks for the reviewers for their constructive comments.

**References**

1. The United Nations World Water Development Report 2014.
2. Observ ER (2013) Electricity production in the world. Fifteenth inventory edition.
3. Li M, Li X (2005) MEP-type distribution function: a better alternative to Weibull function for wind speed distributions. *Renew Energy* 30: 1221-1240.
4. Mathew S, Pandey KP (2003) Modelling the integrated output of wind-driven roto-dynamic pumps. *Renew Energy* 28: 1143-1155.
5. Bataineh KM, Dalalah D (2013) Assessment of wind energy potential for selected areas in Jordan. *Renew Energy* 59: 75-81.
6. Boudia SM, Benmansour A, Ghellai N, Benmedjahed M, Tabet Hellal MA (2013) Temporal assessment of wind energy resource at four locations in Algerian Sahara. *Energy Conversion and Management* 76: 654-664.
7. Omer AM (2008) On the wind energy resources of Sudan. *Renew Sust Energy Rev* 12: 2117-2139.
8. Mouangue RM, Kazet MY, Kuitche A, Ndjaka JM (2014) Influence of the Determination Methods of K and C Parameters on the Ability of Weibull Distribution to Suitably Estimate Wind Potential and Electric Energy. *Int J Renew Energy Develop* 3: 145-154.
9. Ohunakin OS, Akinnawonu OO (2012) Assessment of wind energy potential and the economics of wind power generation in Jos, Plateau State, Nigeria. *Energy Sustain Develop* 16: 78-83.
10. Justus CG, Mikhail A (1976) Height variation of wind speed and wind distributions statistics. *Geophys Res Lett* 3: 261-264.
11. Mathew S, Pandey KP (2000) Modelling the integrated output of mechanical wind pumps. *J Solar Energy Engineering* 122: 203-206.

12. Vestas V29 documentation.
13. Vestas V100 documentation.
14. Carta JA, Ramírez P, Velázquez S (2008) Influence of the level of fit of a density probability function to wind-speed data on the WECS mean power output estimation. *Energy Convers Management* 49: 2647-2655.
15. Eclipse for Parallel Application Developers.
16. Safari B, Gasore JA (2010) Statistical investigation of wind characteristics and wind energy potential based on the Weibull and Rayleigh models in Rwanda. *Renewable Energy* 35: 2874-2880.